Photoreceptors and diurnal variation in spectral sensitivity in the fiddler crab *Gelasimus dampieri*

Anna-Lee Jessop[1,2*], Yuri Ogawa[3+], Zahra M. Bagheri[1,2+], Julian C. Partridge[2] and Jan M. Hemmi[1,2]

[1] School of Biological Sciences, The University of Western Australia, 35 Stirling Highway, Crawley, Western Australia 6009, Australia

[2] UWA Oceans Institute, The University of Western Australia, 35 Stirling Highway, Crawley, Western Australia 6009, Australia

[3] Centre for Neuroscience, Flinders University, GPO Box 2100, 5001 Adelaide, SA, Australia

Corresponding author:

[*]Anna-Lee Jessop

School of Biological Sciences and UWA Oceans Institute, The University of Western Australia, 35 Stirling Highway, Crawley, Western Australia 6009, Australia

Email: anna-lee.jessop@research.uwa.edu.au

[+]These authors contributed equally.

Abstract

Colour signals, and the ability to detect them, are important for many animals and can be vital to their survival and fitness. Fiddler crabs use colour information to detect and recognise conspecifics, but their colour vision capabilities remain unclear. Many studies have attempted to measure their spectral sensitivity and identify contributing retinular cells, but the existing evidence is inconclusive. We used electroretinogram (ERG) measurements and intracellular recordings from retinular cells to estimate the spectral sensitivity of *Gelasimus dampieri* and to track diurnal changes in spectral sensitivity. *G. dampieri* has a broad spectral sensitivity and is most sensitive to wavelengths between 420 to 460 nm. Selective adaptation experiments uncovered an ultraviolet (UV) retinular cell with a peak sensitivity shorter than 360 nm. The species' spectral sensitivity above 400 nm is too broad to be fitted by a single visual pigment and using optical modelling we provide evidence that at least two medium-wavelength sensitive (MWS) visual pigments are contained within a second blue-green sensitive retinular cell. We also found an approximate 25 nm diurnal shift in spectral sensitivity towards longer wavelengths in the evening in both ERG and intracellular recordings. Whether the shift is caused by screening pigment migration or changes in opsin expression remains unclear, but the observation shows the diel dynamism of colour vision in this species. Together, these findings support the notion that *G. dampieri* possesses the minimum requirement for colour vision, with UV and blue/green receptors, and help to explain some of the inconsistent results of previous research.

Keywords:

Spectral sensitivity, Colour vision, Fiddler crab, Retinular cells, Photoreceptors, Ultraviolet

Introduction

To animals that can perceive colour, the natural world is bursting with colour signals. These signals are often vital to an animals' survival and fitness. We know that animals use colour signals to locate food sources (Chittka and Menzel, 1992), in mate choice (Hunt et al., 2001), and in visual communication (reviewed in Osorio and Vorobyev (2008)). How animals perceive these colours entirely depends on the colour vision system with which they are equipped. True colour vision, the ability to discriminate between different wavelengths of light, or different spectral radiance distributions, requires at least two distinct spectral channels. The range of colours that can be discriminated, and the accuracy with which an animal can make colour discriminations, generally increases with increasing spectral channels and the resulting dimensionality of colour space (Kelber et al., 2003).

Fiddler crabs are colourful animals that incorporate many colours in their exoskeletons, with patches on their carapace and appendages variously spanning the regions of human colour space that we categorise as blue, green, yellow, orange, and red (Crane, 1975). These colours are linked to species recognition and intraspecific signalling (Detto, 2007; Detto et al., 2006; Detto and Backwell, 2009). For example, female *Austruca mjoebergi* (Shih et al., 2016) (formerly *Uca mjoebergi*) recognise conspecific males by the colours of their chelae, and prefer males with high UV reflections (Detto, 2007; Detto et al., 2006; Detto and Backwell, 2009). Nevertheless, no studies have provided evidence that fiddler crabs have the required number of spectral channels to discriminate between the various colours they exhibit or between different shades (whether hue, saturation, or brightness) of similar colours, as would be required in mate choice (Horch et al., 2002; Hyatt, 1975; Scott and Mote, 1974). The importance of colour signals in fiddler crab behaviour has prompted investigations into the colour vision system of fiddler crabs (Alkaladi, 2008; Falkowski, 2017; Horch et al., 2002; Hyatt, 1975; Jordão et al., 2007; Rajkumar et al., 2010; Scott and Mote, 1974; Smolka, 2009). Yet despite the considerable effort, some fundamental properties of how these animals see colour, including the number of spectral channels they possess, remain poorly understood. We know that fiddler crabs have a relatively broad spectral sensitivity, extending from around 400 to 600 nm, and are maximally sensitive to the region of the spectrum we describe as blue-green (Horch et al., 2002; Hyatt, 1975; Jordão et al., 2007; Scott and Mote, 1974). The width of their spectral sensitivity suggests that a few visual pigment types are contained within their eyes.

Like most crustaceans, ommatidia in the fiddler crab compound eye are composed of eight retinular cells. These are differentiated into proximal retinular cells (R1–R7) and a small

distal retinular cell (R8) (Alkaladi and Zeil, 2014; Shaw and Stowe, 1982). Each rhabdom is surrounded by a dense layer of screening pigment which spectrally filters light passing down the rhabdom, hence altering the retinular cells' effective spectral sensitivities (Alkaladi and Zeil, 2014; Jordão et al., 2007). Jordão et al. (2007) used microspectrophotometry (MSP) in an attempt to characterise the light absorption of the visual pigments located in the proximal retinular cells (R1–R7) and the screening pigments of four fiddler crab species: *Leptuca pugilator* (formerly *Uca pugilator*), *Minuca pugnax* (formerly *Uca pugnax*), *Afruca tangeri* (formerly *Uca tangeri*), and *Gelasimus vomeris* (formerly *Uca vomeris*) (Shih et al., 2016). Their results suggest a single visual pigment type, absorbing maximally between 525–600 nm, exists in R1–R7 in all four species. Due to the small size of the distal R8, their study was not able to measure the visual pigment in these cells. Furthermore, the high density of screening pigments in fiddler crabs makes it difficult to measure the absorbance spectrum of their visual pigments without some spectral contamination from the surrounding screening pigments.

In contrast, molecular biological techniques have found evidence that at least two visual opsins are expressed in *G. vomeris* (Alkaladi, 2008) and *L. pugilator* (Rajkumar et al., 2010). In *G. vomeris* two opsin genes (*UcaOpsin1* and *UcaOpsin2*) are differentially expressed across the eye (Alkaladi, 2008). In *L. pugilator* the opsin genes *UpRh1* and *UpRh2* appear to be differentially expressed in R1–R7, with one of the retinular cells co-expressing the opsin genes (Rajkumar et al., 2010). In both species, these opsins are predicted to be MWS. In addition, Rajkumar et al. (2010) found in *L. pugilator* that R8 expresses the opsin gene *UpRh3*, which has a similar sequence to UV opsins in other arthropods. Both Rajkumar et al. (2010) and Alkaladi (2008), therefore imply that these species of fiddler crab have the molecular basis for at least dichromatic colour vision. However, these studies do not provide us with direct information about the classes of visual pigments, nor the spectral sensitivity of the retinular cells including the light filtering effects of the screening pigments.

Physiological measurements of fiddler crabs' spectral sensitivities are contradictory and a clear conclusion is still lacking. Three studies have measured the ERG of a number of species of fiddler crabs including *M. pugnax* and *L. pugilator* (Scott and Mote, 1974), and *Leptuca thayeri* (formerly *Uca thayeri*), *M. pugnax, L. pugilator,* and *Minuca minax* (formerly *Uca minax*) (Horch et al., 2002; Hyatt, 1975). Scott and Mote (1974) suggested that both *M. pugnax* and *L. pugilator* possess a single spectral type of retinular cell with a peak sensitivity around 510 nm. However, their study suffered from several methodological limitations (reviewed in Horch et al. (2002)). More recent ERG measurements (Horch et al., 2002; Hyatt,

1975) have implied that at least two distinct spectral types of retinular cells exist in fiddler crab eyes, one long wavelength sensitive (λ_{max} 500–540 nm) and one short wavelength sensitive (λ_{max} 430 nm) though neither study successfully provided conclusive evidence for this.

The discrepancies among all previous studies highlight the difficulty of conclusively defining the spectral types of retinular cells in the fiddler crab eye. Measuring spectral sensitivity of the crabs' retinular cells intracellularly is difficult due to the small size of the crabs' retinular cells, particularly in the case of R8 (Alkaladi and Zeil, 2014; Falkowski, 2017; Smolka, 2009). Additionally, there is some evidence that fiddler crabs possess a complex combination of visual pigments that are highly variable from cell to cell (Alkaladi, 2008; Falkowski, 2017; Rajkumar et al., 2010; Smolka, 2009), making it difficult to classify the spectral types of retinular cells unequivocally. If opsin co-expression does indeed exist within fiddler crab eyes, this is likely to lead to atypically broad spectral sensitivities and associated difficulties when estimating the contribution of different spectral classes of retinular cells to physiological data (Arikawa et al., 2003). Finally, physical and physiological changes within compound eyes can further complicate the matter. Physical changes observed in crustacean eyes include daily changes to opsin concentration within the rhabdom (Battelle, 2013; Katti et al., 2010) and daily movement of the light filtering screening pigments that surround the rhabdom (Olivo and Chrismer, 1980; Olivo and Larsen, 1978; Ribi, 1978; Satoh et al., 2017; Stowe, 1980). Both mechanisms can affect the spectral sensitivity of retinular cells. The movement of screening pigments leads to a shift in peak spectral sensitivity of up to 35 nm in the crayfish (*Orconectes sp.* and *Procambarus sp.*), (Goldsmith, 1978), and up to 40 nm in the moth, *Adoxophyes orana* (Satoh et al., 2017). We also know that the size of the rhabdom can vary throughout the day in a number of related species of crabs (Nässel and Waterman, 1979; Rosenberg et al., 2000; Rosenberg and Langer, 2001; Stowe, 1982; Toh, 1987) and depending on opsin concentration, rhabdomeric size changes may result in variable spectral sensitivity over the day (Katti et al., 2010). Increases in rhabdom length would be predicted to broaden spectral sensitivities (Brindley, 1960), but it is possible for changes in rhabdom width to alter spectral sensitivity too. Diurnal changes in rhabdomeric width have recently been shown for the fiddler crab *A. tangeri* (Brodrick et al., 2020). If waveguide modes vary as a result, it is possible that the contribution of surrounding screening pigments to spectral rhabdomeric absorption could affect the cells' overall spectral sensitivity, with smaller diameter cells predicted to be more affected than larger ones (Van Hateren, 1984). As a further complication, the location of screening pigments within the ommatidia also changes diurnally in the fiddler

crab *L. pugilator* (Fielder et al., 1971; Fingerman, 1970; Reddy et al., 1997). Thus, diel shifts in fiddler crab spectral sensitivities may also be anticipated.

Here, we investigate the spectral sensitivity of the Australasian fiddler crab *Gelasimus dampieri* (Shih et al., 2016) (formerly *Uca dampieri* (Crane, 1975)), using ERGs, single cell intracellular recordings made with sharp electrodes, and an experimental behavioural paradigm based on fiddler crab escape performance. The spectral sensitivity of several simultaneously stimulated ommatidia were measured with ERGs using a method of stimulation that provides an improved signal to noise ratio, with higher spectral resolution and range (down to 350 nm) (Ogawa et al., 2015). By making use of monochromatic adaptation lights during ERG recordings, we were able to suppress the response of specific spectral classes of retinular cells, revealing a distinct UV sensitive retinular cell. Single cell recordings revealed broad blue-green sensitive retinular cells that appear to co-express at least two opsins. Both ERGs and single cell recordings showed shifts in spectral sensitivity, of ~25 nm, towards longer wavelengths over the course of the day. Spectral sensitivity measurements based on the escape response of the crabs supports conclusions made from physiological spectral sensitivity data.

Method

Animals

Fiddler crabs (*G. dampieri* (Crane, 1975)) were collected in daylight at low tide from a mangrove habitat near Learmonth (22°18S, 114°9E), south of Exmouth, Western Australia, in May 2014, April 2015 and July 2017, and from a mangrove habitat near Broome (17°57S, 122°14E) in July 2016. After field collection, crabs were housed in plastic containers with sea water and were transported by car to the University of Western Australia, Perth, WA. There they were housed in an artificial mudflat enclosure with an immersion/emersion tidal cycle in which crabs were immersed in sea water twice daily, under a 12 hour light:12 hour dark cycle (light phase from 6 a.m. till 6 p.m.) and were fed dried flake food (Aqua One© Tropical Flakes) every two days. Selective adaptation experiments were conducted on four male and eight female crabs from the Exmouth collection site. ERGs measuring diurnal changes were conducted on four females and four males from the collection site in Broome. Single cell recordings were made from two male and four female crabs from the collection site in Exmouth. Behavioural experiments were conducted on two males and two females from the Exmouth collection site. Different groups of animals were used for the four different

experiments (two ERG experiments, one intracellular, and one behavioural experiment). No single animal was used across two different experiments.

Electrophysiology

Fiddler crabs were treated according to UWA Animal Ethics Committee (AEC) approved methods (UWA AEC project numbers RA/3/100/1515 and RA/3/400/1020). A fiddler crab was removed from the holding facility and its carapace was glued with LOCTITE® Superglue (ethyl cyanoacrylate) to a small insulated plastic disc that was then glued to a vertical metal rod so that the crab was in its natural posture. Both eyes were stabilised in a natural upright position by gluing the eye stalks to a wooden post as depicted in Figure 1. The crab was then partially submerged in a plastic container filled with sea water and placed in a grounded Faraday cage.

To record the electrophysiological response of the eye to the light stimuli, the ERG was recorded and used to determine the spectral sensitivity of the illuminated equatorial and frontal part of the eye. A 0.254 mm diameter platinum electrode was placed on the cornea of the stimulated compound eye with conductive gel (Livingstone International Pty Ltd., New South Wales, Australia). A shielded silver/silver chloride pellet was placed inside the sea water bath containing the crab and served as the indifferent electrode. The wire placed on the stimulated eye acted as the recording electrode. ERGs were recorded through a differential amplifier (DAM50, World Precision Instruments Inc., FL, USA) connected to a computer via a 16-bit data acquisition card (USB-6353, National Instruments, Austin, TX, USA), with the ground connected to the recording table. Data were acquired at 5 kHz using custom made software in MATLAB 2015B (MathWorks®) and the signal was monitored using an oscilloscope (Tektronix 5223, Tektronix Inc., Beaverton, OR, USA). Measurements were taken across the ultraviolet to visible (UV–VIS) spectrum, taken in sequence from 610 to 350 nm in 20 nm steps and then from 360 to 620 nm in 20 nm steps.

The spectral sensitivities of single retinular cells were determined by intracellular measurements with sharp electrodes. A small incision was made in the cornea at the top of the eye using a razor blade, to provide access to the retinular cells. Microelectrodes (borosilicate glass World Precision Instruments, Inc.; 1.2 mm outer diameter, 0.68 mm inner diameter) were pulled on a laser-based micropipette puller (P-2000, Sutter Instrument, Novato, CA, USA) yielding tip resistances of 40–80 MΩ when filled with 1 M potassium chloride. The electrode was then inserted into the retina through the small hole and served as the recording electrode.

The shielded silver/silver chloride pellet in the sea water bath served as the indifferent electrode. Membrane potentials were recorded via an amplifier (Getting Model 5A, Getting Instruments, San Diego, CA, USA), connected to a computer via the 16-bit data acquisition card (see above). The successful penetration of a retinular cell was indicated by the amplitude of the response to a flash of light. As a criterion for a healthy recording, the response amplitude to a flash of light needed to exceed 15 mV. After penetrating a retinular cell with the electrode, the position of the optical stimulation fibre was adjusted to produce the maximum retinular cell response. Measurements were taken in sequence across the UV–VIS spectrum from 610 to 350 nm in 20 nm steps and then from 360 to 620 nm in 20 nm steps. Crabs were semi-immersed in sea water for the duration of the experiment. Crabs were euthanized at the conclusion of each intracellular recording.

Stimulus

Monochromatic stimulation and adaptation lights were produced by computer-controlled monochromators (TILL Polychrome V, Till Photonics GmbH, Gräfelfing, Germany) illuminated with 150 W xenon lamps (USHIO Xenon Short Arc Lamp UXL-150S, Ushio America Inc., CA, USA). White light, with a range from 185 to 2000 nm, (Fig. S1) was provided by a 35 W xenon light source (HPX-2000, Ocean Optics Inc., FL, USA). Our light stimulation protocol is similar to that described by (Ogawa et al., 2015). To investigate visual spectral sensitivities a flickering light stimulus was used, alternating with a 50% duty cycle between light and dark at a frequency of 10 Hz. The light phase alternated between monochromatic and white light illumination. The angular size of the circular stimulus (aperture of the lens) was approximately 1.5° in diameter when viewed by a crab positioned at the centre of the recording setup (15 cm away from the light). Therefore, based on estimated interommatidial angles (1.25° and 0.26°, horizontal and vertical, respectively) in *G. dampieri* (Bagheri et al., 2020), approximately 8–12 ommatidia or 64–72 retinular cells viewed at least part of the aperture when the centre of the eye was stimulated. Examples of a raw ERG recording and a filtered intracellular recording are shown in the Supplementary Material (Fig. S2). The white light intensity was invariant but, at each wavelength tested, the intensity of the monochromatic light was adjusted to produce the same electrophysiologically measured response amplitude from the monochromatic light to dark transition as that produced by the white light to dark transition. By comparing the photon irradiance of monochromatic light, of different wavelengths, required to match the photon irradiance of white light allowed us to calculate the crab's relative spectral sensitivity for all measured wavelengths. Additionally, we

calculated the mean amplitude of the response to the standard white light to dark transition throughout each recording to provide a way of comparing response amplitudes across crabs.

Two different ERG experiments were conducted to investigate the spectral types of retinular cells contributing to the spectral sensitivity of *G. dampieri*. In the 'Adaptation Experiments', the eye was illuminated with an additional monochromatic adaptation light to reduce the contribution to the measured signal from some retinular cell classes by reducing their effective stimulus contrast. Adaptation lights were delivered through a beam splitter to achieve exact spatial alignment with the stimulus light. Adaptation lights had a bandwidth of 15 nm (full width at half maximum transmission) and peaked at 420 nm, 430 nm, or 530 nm. Irradiance measurements of the adaptation lights and the invariant white light were made using an ILT1700 radiometer and SED033 detector (International Light Technologies Inc., MA, USA). The brightest possible irradiance of each adaptation light was used in all 'Adaptation Experiments'. Eight female and four male crabs were used in the 'Adaptation Experiments', however not all crabs were measured in all conditions. In the 'Time of Day Experiments' we examined whether the spectral sensitivity of the crabs varied predictably across the day. Spectral sensitivities were measured by recording ERGs at four different times during the day: 9 a.m., 12 p.m., 3 p.m. and 6 p.m. Using a Latin Square design, the spectral sensitivity of each fiddler crab was measured at all four times in a pseudo-random order. We measured four females and four males, and all crabs were measured at each time point. Measurement duration was approximately 20 minutes and the average stimulus intensity remained constant at each time point.

Optical model for the fiddler crab ommatidium

To estimate the number of spectral types, and describe the spectral absorption characteristics of the retinular cells in *G. dampieri*, an optical model was adapted based on the approach of Stavenga and Arikawa (2011). Visual pigment normalised absorbance spectra ($\boldsymbol{a_i(\lambda)}$) were calculated using the A1 chromophore Govardovskii template (Govardovskii et al., 2000). The absorbance spectrum of ommatidial lateral screening pigments ($\boldsymbol{a_s(\lambda)}$) was taken from Jordão et al. (2007) who measured it in the closely related species *G. vomeris* (Fig. 1B). On the basis of anatomical details of the fiddler crab ommatidia reported by Alkaladi and Zeil (2014) we made the following assumptions: (1) The total length ($\mathbf{z}$) of the rhabdom was 350 μm; (2) The lateral screening pigment extended the entire length of the rhabdom; (3) The peak Napierian absorbance coefficient of the visual pigments was 0.0067 μm^{-1} (Cronin and Forward Jr, 1988). These values were incorporated into a simple model in which the wave-optical properties of

the rhabdom were simplified, the model assumed that light entering the rhabdom propagates entirely inside the rhabdom and that the lateral screening pigment exerts its filtering action as if it was within the rhabdom (Stavenga and Arikawa (2011)). The spectral transmittance ($\boldsymbol{T(\lambda)}$) of a thin ($\Delta \mathbf{z}$ = 1 μm) section of the rhabdom at any point along its length, is then given by:

$$\boldsymbol{T(\lambda) = exp(-k(\lambda)\Delta z)} \quad \textbf{(1)}$$

where:

$$\boldsymbol{k(\lambda) = k_v(\lambda) + k_s(\lambda)} \quad \textbf{(2)}$$

and where $\boldsymbol{k_v(\lambda)}$ is the Napierian spectral absorbance coefficient of the visual pigments given by:

$$\boldsymbol{k_v(\lambda) = k_{v,max}\left\{\sum a_i(\lambda)\, p_i\right\}} \quad \textbf{(3)}$$

with $\boldsymbol{k_{v,max}}$ the peak Napierian absorbance coefficient of the visual pigments, $\boldsymbol{a_i(\lambda)}$ the normalised absorbance spectrum of the visual pigments, and $\boldsymbol{p_i}$ the relative occupancy of the (putative) different visual pigment types within the rhabdom where $\boldsymbol{i}$ is between one and the number of visual pigments incorporated into the model, and:

$$\boldsymbol{k_s(\lambda) = k_{s,max} a_s(\lambda)} \quad \textbf{(4)}$$

with $\boldsymbol{k_{s,max}}$ being the peak absorbance coefficient of the screening pigment and $\boldsymbol{a_s(\lambda)}$ the normalised absorbance spectrum of the screening pigment (Fig. 1B). The light flux at location $\boldsymbol{z}$, $\boldsymbol{I(z,\lambda)}$, then changes to $\boldsymbol{I(z+\Delta z,\lambda)}$, the light flux at location $\boldsymbol{z+\Delta z}$, as:

$$\boldsymbol{I(z+\Delta z,\lambda) = T(\lambda) I(z,\lambda).} \quad \textbf{(5)}$$

The spectral light flux $\boldsymbol{\Delta A_i(\lambda)}$ absorbed by the visual pigment within rhabdomal thickness element $\boldsymbol{\Delta z}$ is given by

$$\boldsymbol{\Delta A_i(\lambda) = [I(z,\lambda) - I(z+\Delta z,\lambda)] k_{v,max} a_i(\lambda) p_i / k(\lambda).} \quad \textbf{(6)}$$

Summing the absorbed light fraction of the retinular cells over the different rhabdom compartments and dividing that by the incident light, $\boldsymbol{I_0(\lambda)}$, yields the retinular cells' absorptance spectrum. The number of rhabdom compartments is equal to the length of the rhabdom divided by $\boldsymbol{\Delta z}$ (1 μm); in our modelling there were 350 compartments.

The absorptance spectrum was fitted to the scaled spectral sensitivity data from physiological recordings over the wavelength range 400 nm to 600 nm due to the lack of data below 400 nm in the screening pigment template. By minimizing the root mean square difference between the

modelled data and the ERG recordings we were able to determine the best fitting visual pigment λ_{max} values, their relative occupancies (relative contribution) ($\boldsymbol{p_i}$), and the peak absorbance coefficient of the screening pigment ($\boldsymbol{k_{s,max}}$). To explore certain hypotheses these parameters could be constrained or unconstrained. As previously mentioned, the rhabdom of fiddler crabs is surrounded by a dense layer of screening pigment (Alkaladi and Zeil, 2014; Jordão et al., 2007), therefore, when fitting the optical model to our physiological data, a screening pigment template was always included in the model. The exclusion or inclusion of the screening pigment template did not greatly affect the model result (Supplementary Material, Fig. S3). When comparing models with the same number of unconstrained parameters we compared the sum of squares between the models to identify the best-fitting model. When comparing models with different numbers of unconstrained parameters an F-test was performed to test the level of improvement in the fit between models (Anderson and Conder, 2011). Models were fitted to the data of ERG experiments independently as the crabs used in each experiment came from geographically distinct populations separated by ~1200 km. The intracellular data came from crabs from the same population as the 'Selective Adaptation' experiment, models were again fitted to these data sets independently due to the difference in methodologies.

Effective contrast calculation

We calculated the absorption of incident light during stimulation by each modelled visual pigment. The absorption of incident light provided by the adaptation light alone and the sum of the white light and adaptation light were used to calculate the effective Michelson's contrasts that each modelled visual pigment would have experienced during experimental stimulation. The irradiance of the 420, 430, and 530 nm adaptation lights were 0.55, 0.60, and 0.76 µmol m^{-2} s^{-1}, respectively, and the irradiance of the invariant white light was 0.16 µmol m^{-2} s^{-1}. Assuming the full effect of the measured intensity of the adaptation light on the visual pigments, the Michelson's contrast is defined as:

$$\frac{\boldsymbol{I_{max}} - \boldsymbol{I_{min}}}{\boldsymbol{I_{max}} + \boldsymbol{I_{min}}} \tag{7}$$

with $\boldsymbol{I_{max}}$ and $\boldsymbol{I_{min}}$ representing the highest and lowest luminance, respectively. In this case $\boldsymbol{I_{max}}$ is the sum of the photon flux of the white light and adaptation light and $\boldsymbol{I_{min}}$ is the photon flux of the adaptation light alone.

Behavioural spectral sensitivity

The behavioural apparatus consisted of a treadmill setup similar to that described by How et al. (2012). A 100 mm diameter polystyrene ball balanced on a cushion of air flowing from a reservoir was used as the treadmill. The crab was fixed in position on top of the treadmill using a small metal rod fixed to the carapace of the crab. The rod was attached to a pivot system allowing the crab to rotate about the vertical axis and to walk freely in any direction along the surface of the treadmill. The treadmill was placed in the middle of a testing arena (53.5x53.5 cm) where the floor was level with the top of the treadmill which was surrounded by three liquid crystal display (LCD) monitors (33x51 cm; DELL 90-130, Ireland) and one white diffusing screen. LCD monitors showed a stationary image, simulating a mudflat with a dark ground and a bright sky, providing a steady but dim background light. The stimulus light was delivered from a computer controlled monochromator (as above) via an optical fibre and imaged through a lens before passing through a neutral density (ND) filter, a motorised aperture, and finally projected onto the white diffusing screen from a distance of approximately 920 mm. The background of the white diffusing screen was not illuminated. The resulting stimulus was an expanding, circular monochromatic light, which mimicked a sphere approaching the crab along a straight line on a direct collision course. The motorised aperture, was controlled by a stepper motor. The angular size of the stimulus exponentially increased from 2.1° to 23.9° over three seconds.

Each animal was mounted on the treadmill and allowed 3–5 minutes to acclimatise. A stimulus of a given wavelength and intensity was then presented and the crab's response recorded. Crab behaviour and stimulus events were recorded using a high definition (HD) digital (1920x1080 pixels) video camera (Handycam HDR-CX550, SONY, Japan) recording at 25 frames per second located directly above the testing arena. To prevent habituation, each crab was presented with only three trials every two days (Tomsic et al., 1998). Video recordings were analysed after each trial to determine if stimuli resulted in an escape response. Test wavelengths included: 360 nm, 380 nm, 400 nm, 420 nm, 440 nm, 460 nm, 480 nm, 500 nm, 540 nm, and 600 nm. Each crab was randomly assigned an order of test wavelengths.

The ND filters inserted into the light path and the exit slit of the monochromator were used to change the intensity of the stimulation. The stimulus radiance (μmol $m^{-2}sr^{-1}$) was measured using an ILT1700 light spectrometer (International Light Technologies Inc., MA, USA) that was positioned at the crabs' location in front of the diffusing screen. At each wavelength the maximum intensity was recorded. Monochromator exit slits and ND filter

combinations were found to produce decreasing intensities in a logarithmic fashion with a step size of 25% and 19 possible steps beginning from step one (100% intensity) and decreasing to step 19 (0.56% intensity). A modified staircase procedure was used to determine the minimum stimulus intensity needed to elicit an escape response. For each test wavelength the staircase procedure began with step one and if the crab responded within four presentations the intensity was decreased by four steps (31.64% intensity) and the stimulus was re-presented. Intensities were decreased in steps of four until the crab failed to respond to four presentations of the same intensity. Once this occurred, the intensity was then increased by two steps and depending on the response outcome the intensity was either increased or decreased by one step. This procedure would continue until a one-step intensity difference resulted in a different response outcome. The higher intensity of the one-step intensity difference was reported as the threshold intensity for that wavelength. Using the inverse of the threshold values we then produced a relative spectral sensitivity curve. If the full intensity was presented four times with no response, we concluded the animal was not sensitive to that wavelength and the relative spectral sensitivity for that wavelength was zero. Control stimulations, where the light was blocked by a black plastic shield, were presented at regular intervals (every fifth presentation) to ensure potential unintended stimuli, such as any vibrations from the motorised aperture, were not affecting the response.

Results

Estimates of spectral sensitivities of retinular cells

Electroretinogram measurements in *G. dampieri* showed relatively broad spectral sensitivities peaking between 420–460 nm (Fig. 2). There was no difference between the sensitivities of male and female crabs, therefore both sexes were combined in the mean data. Optical models including two visual pigments (Fig. 2B) fit the ERG recordings significantly better than models including a single visual pigment (Fig. 2A) ($F = 54.36$, $p < 0.05$). The best fitting model to the mean ERG data (Fig. 2B) includes visual pigments with λ_{max} values of 431 nm (VP1) and 482 nm (VP2), with relative occupancies (or contributions) ($\boldsymbol{p_i}$) of 0.53 and 0.47, respectively. The screening pigment absorbance coefficient in this model was 0.07 (Fig. 2B).

To separate the responses of distinct spectral classes of retinular cells, adaptation lights were used concurrently with the stimulation lights. When adapted with 420 nm or 430 nm light, the peak spectral response of the fiddler crab eye shifted from ca. 440 nm to between 350 nm and 360 nm (Fig. 2C). An increase in relative sensitivity was seen from 350 nm to 390 nm under

both 420 nm and 430 nm adaptation conditions, however the relative sensitivity from 400 nm to 600 nm was largely unchanged between the 420 nm, 430 nm and no adaptation conditions. Adding a 530 nm adaptation light did not produce a shift in peak sensitivity and only slightly decreased the sensitivity around 500 nm of the stimulated ommatidia (Fig. 2D).

To further investigate the effect of each adaptation light, we fitted the model from Fig. 2B to the spectral responses of each adaptation condition, leaving the λ_{max} of each visual pigment and the screening pigment absorbance coefficient constrained, but allowing the relative contribution of the visual pigments to vary. The λ_{max} of each visual pigment was constrained to 431 nm for VP1 and 482 nm for VP2. The screening pigment absorbance coefficient was constrained to 0.07. Despite the strong adaptation lights, the relative contribution of the two visual pigments varied only slightly (between 5 and 15%) compared to the no adaptation light condition (Table 1).

Calculated contrast values show that the contrast 'seen' by putative visual pigments would have varied very strongly under the different adaptation conditions if they were functionally independent (Table 2), but the model-estimated visual pigment contributions remained almost completely stable as seen in Table 1. In other arthropods minimum contrast thresholds to elicit a response from a retinular cell are between 2.5–6% (O'Carroll and Wiederman, 2014; Ogawa et al., 2019; Ryan et al., 2020) and in *G. dampieri* it is predicted to be approximately 3% (Z.M. Bagheri, unpublished data). If we assume each visual pigment is contained within a discrete retinular cell, then we would expect to see no response to the 10 Hz stimulation from the retinular cells under adaptation conditions where the contrast 'seen' was below 2.5%, leading to a significant change in the relative contributions of modelled visual pigments. In all adaptation conditions, however, this was not the case, and modelled relative contributions remained similar to the no adaptation model. Even though the recorded spectral sensitivity remained mostly unchanged, we have clear evidence that the adaptation lights were visible to the crabs. The 420 nm, 430 nm and 530 nm adaptation lights reduced the amplitudes of responses to the standard white light to dark transition to (respectively) 48.9%, 52.5% and 74.6% of the amplitude recorded under conditions of no adaptation. In addition, the strong UV component of the spectral response unveiled under 420 nm and 430 nm adaptation lights (Fig. 2C) clearly highlights the effectiveness of these shortwave adaptation lights. Under 530 nm adaptation the strong UV response component was not seen. If we assume the 431 nm and 482 nm visual pigments are contained within the same retinular cell, then we may expect this to be

the case. For this putative retinular cell, the calculated perceived contrast was twice as high under the 530 nm adaptation condition compared to the other adaptation conditions, indicating that the adaptation effect of the 530 nm light was weaker compared to the other adaptation conditions.

Diurnal changes in spectral sensitivity

Electroretinogram recordings were taken from eight *G. dampieri*, four females and four males, at four different times of day: 9 a.m., 12 p.m., 3 p.m. and 6 p.m. Fig. 3A displays the mean ERG data recorded at each time, fitted with optical models. A clear shift in spectral sensitivities towards longer wavelengths later in the day can be seen and this is quantified by the optical model results in Table 3. The peak sensitivity at 9 a.m. shifted by approximately 25 nm towards longer wavelengths by 6 p.m.

In order to understand the possible causes of this shift, three different hypotheses were compared: (1) the migration of the screening pigments that surround the rhabdom is causing the shift; (2) differential regulation of opsin co-expression is causing the shift; and (3) the combined effect of the migration of screening pigments and the differential regulation of opsin co-expression are causing the shift. To test these three hypotheses the ERG data recorded at different times of day were combined and fitted with a model that best fitted all data, as shown in Fig. 3B. This model included two visual pigments with λ_{max} values of 454 nm (VP1) and 496 nm (VP2) and relative contributions of 0.73 and 0.27, respectively, with a screening pigment having an absorbance coefficient of 0.005. This model was then fitted to the ERG data from each time of day separately with the following constraints: (1) (Screening pigment migration) the screening pigment absorbance coefficient ($\boldsymbol{k_{s,max}}$) was unconstrained but all other parameters were constrained to the results from the best fitting model, (2) (Opsin regulation) the relative contributions of visual pigments ($\boldsymbol{p_i}$) were unconstrained with all other parameters constrained, and (3) (Combination) all parameters were unconstrained except the λ_{max} for each visual pigment. The sum of squares between the data and the models were compared between each hypothesis (Fig. 3C), however no clear difference was found. The ERG data fit with each model and the best fitting parameters for each model are shown in the Supplementary Material (Fig. S4 and Table S1).

Single cell recordings

The spectral sensitivities of 19 retinular cells were measured intracellularly using sharp electrodes between 12 p.m. and 7 p.m. (Fig. 4A). During one single cell recording (Cell 19), we were able to hold the cell over approximately three hours which permitted measurement of spectral sensitivity from the same cell at two different time points: 1:00 p.m. and 3:51 p.m. (Figure 4b). A clear shift in spectral sensitivity towards longer wavelengths can be seen in this cell, with the peak shifting approximately 20 nm and the width of curve increasing during the three hour time period. Of the remaining 18 recordings, there were two distinct temporal groups, with one group of cells recorded between 12 p.m. and 2 p.m. (early cells, N = 5) (Figure 4c) and a second group between 3 p.m. and 7 p.m. (late cells, N = 13) (Figure 4e). The peaks of the cells recorded from later in the day were shifted towards longer wavelengths by approximately 20 nm compared to the peaks of cells recorded from earlier in the day. All response curves were broad and had similar widths and peaks, depending on time, to the ERG-measured response curves.

A model including two visual pigments and a screening pigment was fitted to the spectral responses of retinular cells measured early (Fig. 4C), late (Fig. 4E), and to the responses from Cell 19 at each time point (Fig. 4D and Fig. 4F). Visual pigment contributions and the screening pigment absorbance coefficients were left unconstrained. The best fitting model parameters show that the relative contributions ($\boldsymbol{p_i}$) of the 486 nm visual pigment increased with time in both data sets (Table 4).

Behavioural spectral sensitivity

During the behavioural spectral sensitivity experiment, an escape response was recorded when a crab ran away from the looming stimulus. Of the trials where an escape run was elicited, crabs consistently sprinted directly away from the stimulus (Fig. 5A, Rayleigh test, N = 24, $p<0.01$). The spectral sensitivity estimate from this experiment has a peak sensitivity of approximately 460 nm and decreases both towards shorter and longer wavelengths (Fig. 5B). Crabs were tested between 9 a.m. and 5 p.m., however due to the experimental design and issues relating to habituation, it was not possible to test the effect of time of day on spectral sensitivity.

Discussion

Our results show that the fiddler crab *G. dampieri* possesses at least two spectrally distinct types of retinular cells, with peak sensitivities in the UV and blue-green region of the spectrum. The blue-green sensitive retinular cells appear to contain at least two visual pigments and the measured spectral sensitivity shifts to longer wavelengths over the course of the day. Preliminary spectral sensitivity estimates based on the fiddler crabs escape behaviour support the physiological spectral sensitivity measurements.

UV sensitive retinular cell

The finding of a UV-sensitive retinular cell in our selective adaptation experiments (Fig. 2C) is consistent with two previous studies. Rajkumar et al. (2010) provided evidence that *L. pugilator* expresses an apparent UV-sensitive (UVS) opsin in R8 and Detto and Backwell (2009) showed that the fiddler crab, *A. mjoebergi* can use UV cues in mate choice. The preliminary results from our behavioural experiment also support this finding, with two crabs responding to test wavelengths of 360 nm and 380 nm. We were unable to record intracellularly from the UV sensitive retinular cell and therefore cannot be sure about the exact wavelength of its peak sensitivity, but we estimate it is shorter than 360 nm. The evidence provided in our selective adaption experiments is the first physiological evidence for a UV sensitive retinular cell in fiddler crabs.

Blue-green sensitive retinular cells contain at least two visual pigments

The widths of the spectral sensitivity curves from both our ERG and single cell recordings suggest the blue-green wavelength sensitive retinular cells contain at least two visual pigment types and this is supported by the optical modelling (Fig. 2 and Fig. 4). An important consideration is that the screening pigment absorbance template included in our modelling was measured from *G. vomeris* and not *G. dampieri* (Jordão et al., 2007). However, the two species are very closely related (Shih et al., 2016) and the presence or absence of the screening pigment did not change the conclusion that at least two visual pigment types are contained within the blue-green sensitive retinular cells (e.g. Supplementary Material, Fig. S3). It is possible, though, that the template used in our modelling is not representative of the spectral absorption of *G. dampieri* screening pigment and such measurements should be considered in future research. A second piece of evidence for a two visual pigment retinular cell comes from our ERG recordings that show that the spectral responses to wavelengths between 400–600 nm remained mostly unchanged under all adaptation conditions. Given the effective contrast calculated for the putative VP2 (482 nm) under all adaptation conditions was below the

threshold contrast for most arthropods (Table 2), we would have expected a significant reduction of responses to wavelengths between 500–600 nm if VP2 and VP1 were contained within distinct retinular cells. This was not the case, suggesting the effects of the adapting lights were either overestimated or that two visual pigments are contained within a single retinular cell. The adapting lights did not completely suppress the response of the main population of retinular cells, but we saw a clear effect of the adapting lights on the amplitude of the ERGs and the 420–430 nm adapting lights were strong enough to unveil the UV-sensitive retinular cell (Fig. 2C). Why we did not see a strong increase in the UV response under 530 nm adaptation may be explained by the effective contrast 'seen' by a putative retinular cell containing two visual pigments under 530 nm adaptation. The contrast seen under 530 nm adaptation was double that under 420 nm and 430 nm adaptation. The results from Ogawa et al. (2015), which used the same equipment, show clear effects of different adaptation lights on the spectral responses from Australian bull ants *Myrmecia vindex* and *Myrmecia croslandi*. Specifically, when using a 560 nm adaptation light the spectral responses between 450–600 nm of these ants were drastically reduced (Ogawa et al., 2015). In contrast, in our 530 nm adaptation recordings the reduction in spectral responses was minimal. Furthermore, previous ERG studies also reported no significant difference in spectral response curves when adapting lights between 500 nm and 600 nm were applied (Horch et al., 2002; Hyatt, 1975; Scott and Mote, 1974). Therefore, it seems likely that co-expression of at least two opsins within the blue-green retinular cells explains these results. These findings corroborate some of the results from the molecular biological studies of Alkaladi (2008) and Rajkumar et al. (2010), who found co-expression of MWS opsins in some, but not all, retinular cells. If there were a small number of pure retinular cells, such an arrangement could possibly explain the subtle shifts in our data. However, a simpler explanation of the subtle effects of the adaptation lights would be small differences in the ratio of the two opsins in different cells. In this situation, adaptation lights would change the contribution of those cells to the final recording, thereby leading to small shifts in the sensitivity (Fig. 2).

Our modelling suggests there is a combination of at least two different MWS visual pigments that underlie sensitivity between 400–600 nm and that it may depend on the population of crabs that was measured. For crabs collected from the Exmouth field site one MWS visual pigment has a λ_{max} between 431 nm and 438 nm, and a second MWS visual pigment has a λ_{max} between 482 nm and 486 nm. For crabs collected from the Broome field site the λ_{max} values were longer with one MWS visual pigment λ_{max} of 454 nm and the other 498 nm. Broome and Exmouth are

separated by a considerable distance, approximately 1200 km. The differences between populations were an interesting result and need to be further investigated. On average, across all experiments where spectral sensitivity was measured at approximately 12 p.m. the λ_{max} values of the modelled MWS visual pigments were 438 nm and 484 nm. Our visual pigment λ_{max} estimates are roughly congruent with the predictions from Horch et al. (2002) who suggested the presence of two visual pigments: one with a λ_{max} near 430 nm and the other with a λ_{max} between 500 nm and 540 nm in *L. thayeri*. Furthermore, the peak sensitivity and widths of the spectral response curves from Horch et al. (2002) are very similar to our spectral response curves from later in the day. The MWS visual pigment from Horch et al. (2002) has a slightly longer peak wavelength than our predictions, but their study used a different species of fiddler crab and did not account for lateral screening pigment effects.

Diurnal shifts in spectral sensitivity

In the present study we found diurnal shifts in the spectral sensitivity of the fiddler crab, *G. dampieri*, in both ERG (Fig. 3) and intracellular recordings (Fig. 4). These shifts appear to be endogenous as the adaptation state of the crab remained the same throughout the measurement period. Using modelling we have attempted to explain the cause of this shift (Supplementary Material Fig. S4 and Table S1), however a conclusive explanation remains elusive (Fig. 3C). There are a number of possible explanations for this shift. In this study we focused on the migration of screening pigments that has been shown to occur in *L. pugilator* (Fielder et al., 1971; Fingerman, 1970; Reddy et al., 1997) and differential regulation of opsin gene expression (DeLeo and Bracken - Grissom, 2020; Katti et al., 2010). While the latter has no evidence to occur in fiddler crabs, there is evidence to suggest that the rhabdom width of the fiddler crab *A. tangeri* does fluctuate diurnally (Brodrick et al., 2020). The possibility of a shift in spectral sensitivity due to A1 to A2 chromophore lability was not modelled in our study as no brachyuran crab has been shown to utilise A2-based porphyropsin visual pigments (Cronin and Forward Jr, 1988). To address the question of what is causing the shift in spectral sensitivity observed in *G. dampieri* further research is needed that is beyond the scope of this study.

Ecological relevance of UV/blue-green colour vision

Our findings support the idea that fiddler crabs possess the minimum requirement for colour vision: two spectrally distinct retinular cells, containing three different visual pigments, one UVS (≤360 nm) and two MWS (~438 nm and ~484 nm). Both Detto (2007) and Hyatt (1975) demonstrated colour vision in fiddler crabs and showed that they are able to discriminate between two objects based only upon differences in the spectral distribution of their reflections

and we have now provided the physiological basis for their findings. With this colour vision system, *G. dampieri* would be able to distinguish UV reflections from almost any other background reflection. Specular reflectance measurements have revealed that the white and blue parts of the *G. vomeris* cuticle are highly reflective in the UV region of the spectrum (Hemmi et al., 2006; Zeil and Hofmann, 2001). Very similar patterns of colours are seen in *G. dampieri* (Crane, 1975; Shih et al., 2016) and to a UV/blue-green colour vision system the blue and white patches provide strong contrast signals against the dark mudflat background (Zeil and Hofmann, 2001). These signals would increase the conspicuousness of conspecifics, allowing *G. dampieri* to more easily detect conspecifics for a range of different functions (Zeil and Hofmann, 2001).

Surprisingly, our results, like the results of all previous studies (e.g. Horch et al. (2002), Hyatt (1975), Jordão et al. (2007), and Rajkumar et al. (2010)) suggest that, despite the frequent display of yellow, orange, and red colours (Crane, 1975), fiddler crabs do not possess two distinct spectral channels that would easily discriminate between these colours which differ most in the longwave components of their spectral reflections. Notably, such patterns of colours on the *G. dampieri* carapace and claws reflect in the orange/red region of the spectrum. Furthermore, the carapace colours of other species such as *Tubuca flammula* (formerly *Uca flammula*) are sometimes exclusively red and black. It is possible that small variations in opsin ratios between cells, or a small subset of retinular cells with narrow band spectral sensitivity, could provide these animals with a limited ability to discriminate between some long-wavelength colours if the signals from these retinular cells were kept separated for higher level neural processing. Such small variations would also explain the very small shifts we have observed with our adaptation lights (Fig. 2). The apparent discrepancy between the colour signals displayed by fiddler crabs and their colour vision system offers an interesting challenge to better understand the evolution of colour signals and colour vision systems.

Acknowledgements

We would like to thank Nicolas Nagloo and Marcin Falkowski for their contributions in designing and constructing the equipment used to produce the visual stimuli. We would also like to thank the two anonymous reviewers for their thoughtful and insightful comments on this manuscript.

Competing Interests

The authors declare no competing interests.

Author Contributions

Conceptualization: J.M.H., A.L.J., Y.O.; Methodology: J.M.H., A.L.J., Y.O.; Software: J.M.H., A.L.J., Y.O., Formal Analysis: J.M.H., A.L.J, J.C.P.; Investigation: A.L.J., Z.M.B.; Writing – original: A.L.J.; Writing – review & editing: J.M.H., Y.O., Z.M.B., J.C.P.

Funding

This research was supported under the Australian Research Council Discovery Projects funding scheme (project number DP160102658 and DP180100491) and the Japanese Society for the Promotion of Science (JSPS) postdoctoral fellowship for research abroad to Y.O.

References

Alkaladi, A. and Zeil, J. (2014). Functional anatomy of the fiddler crab compound eye (Uca vomeris: Ocypodidae, Brachyura, Decapoda). *J. Comp. Neurol.* **522**, 1264-1283.

Alkaladi, A. S. (2008). The functional anatomy of the fiddler crab compound eye. *PhD Thesis*, Australian National University, Canberra, ACT.

Anderson, K. B. and Conder, J. A. (2011). Discussion of multicyclic Hubbert modeling as a method for forecasting future petroleum production. *Energy & Fuels* **25**, 1578-1584.

Arikawa, K., Mizuno, S., Kinoshita, M. and Stavenga, D. G. (2003). Coexpression of two visual pigments in a photoreceptor causes an abnormally broad spectral sensitivity in the eye of the butterfly Papilio xuthus. *J. Neurosci.* **23**, 4527-4532.

Bagheri, Z. M., Jessop, A.-L., Kato, S., Partridge, J. C., Shaw, J., Ogawa, Y. and Hemmi, J. M. (2020). A new method for mapping spatial resolution in compound eyes suggests two visual streaks in fiddler crabs. *J. Exp. Biol.* **223**.

Battelle, B. A. (2013). What the clock tells the eye: lessons from an ancient arthropod. *Integr. Comp. Biol.* **53**, 144-153.

Brindley, G. S. (1960). Physiology of the retina and the visual pathway.

Brodrick, E. A., Roberts, N. W., Sumner - Rooney, L., Schlepütz, C. M. and How, M. J. (2020). Light adaptation mechanisms in the eye of the fiddler crab Afruca tangeri. *J. Comp. Neurol.*

Chittka, L. and Menzel, R. (1992). The evolutionary adaptation of flower colours and the insect pollinators' colour vision. *Journal of Comparative Physiology A* **171**, 171-181.

Crane, J. (1975). *Fiddler crabs of the world (Ocypodidae: Genus Uca)*. Princeton, New Jersey: Princeton University Press.

Cronin, T. W. and Forward Jr, R. B. (1988). The visual pigments of crabs. *J. Comp. Physiol., A* **162**, 463-478.

DeLeo, D. M. and Bracken - Grissom, H. D. (2020). Illuminating the impact of diel vertical migration on visual gene expression in deep - sea shrimp. *Mol. Ecol.*

Detto, T. (2007). The fiddler crab Uca mjoebergi uses colour vision in mate choice. *Proc R Soc Biol Sci Ser B* **274**, 2785-2790.

Detto, T., Backwell, P. R., Hemmi, J. M. and Zeil, J. (2006). Visually mediated species and neighbour recognition in fiddler crabs (Uca mjoebergi and Uca capricornis). *Proc R Soc Biol Sci Ser B* **273**, 1661-1666.

Detto, T. and Backwell, P. R. Y. (2009). The fiddler crab Uca mjoebergi uses ultraviolet cues in mate choice but not aggressive interactions. *Anim. Behav.* **78**, 407-411.

Falkowski, M. (2017). The spectral and temporal properties of fiddler crab photoreceptors in the context of predator avoidance. *PhD thesis*, Australian National University Canberra, ACT.

Fielder, D., Rao, K. R. and Fingerman, M. (1971). Control of distal retinal pigment migration in the fiddler crab Uca pugilator. *Marine Biology* **9**, 219-223.

Fingerman, M. (1970). Circadian rhythm of distal retinal pigment migration in the fiddler crab, Uca pugilator, maintained in constant darkness and its endocrine control. *Biol. Rhythm Res.* **1**, 115-121.

Goldsmith, T. H. (1978). The effects of screening pigments on the spectral sensitivity of some Crustacea with scotopic (superposition) eyes. *Vision Res.* **18**, 475-482.

Hemmi, J. M., Marshall, J., Pix, W., Vorobyev, M. and Zeil, J. (2006). The variable colours of the fiddler crab Uca vomeris and their relation to background and predation. *J. Exp. Biol.* **209**, 4140-4153.

Horch, K., Salmon, M. and Forward, R. (2002). Evidence for a two pigment visual system in the fiddler crab, Uca thayeri. *J. Comp. Physiol., A* **188**, 493-499.

How, M. J., Pignatelli, V., Temple, S. E., Marshall, N. J. and Hemmi, J. M. (2012). High e-vector acuity in the polarisation vision system of the fiddler crab Uca vomeris. *The Journal of experimental biology* **215**, 2128-2134.

Hunt, S., Cuthill, I. C., Bennett, A. T. D., Church, S. C. and Partridge, J. C. (2001). Is the ultraviolet waveband a special communication channel in avian mate choice? *J. Exp. Biol.* **204**, 2499-2507.

Hyatt, G. W. (1975). Physiological and behavioural evidence for colour discrimination by fiddler crabs (Brachyura, Ocypodidae, genus Uca). In *Physiological Ecology of Estuarine Organisms*, pp. 333-365. Columbia: University of South Carolina Press.

Jordão, J. M., Cronin, T. W. and Oliveira, R. F. (2007). Spectral sensitivity of four species of fiddler crabs (Uca pugnax, Uca pugilator, Uca vomeris and Uca tangeri) measured by in situ microspectrophotometry. *J. Exp. Biol.* **210**, 447-453.

Katti, C., Kempler, K., Porter, M. L., Legg, A., Gonzalez, R., Garcia-Rivera, E., Dugger, D. and Battelle, B. A. (2010). Opsin co-expression in Limulus photoreceptors: differential regulation by light and a circadian clock. *J. Exp. Biol.* **213**, 2589-2601.

Kelber, A., Vorobyev, M. and Osorio, D. (2003). Animal colour vision–behavioural tests and physiological concepts. *Biological Reviews* **78**, 81-118.

Nässel, D. R. and Waterman, T. H. (1979). Massive diurnally modulated photoreceptor membrane turnover in crab light and dark adaptation. *J. Comp. Physiol., A* **131**, 205-216.

O'Carroll, D., C. and Wiederman, S., D. . (2014). Contrast sensitivity and the detection of moving patterns and features. *Philos Trans R Soc Lond B Biol Sci* **369**, 20130043.

Ogawa, Y., Falkowski, M., Narendra, A., Zeil, J. and Hemmi, J. M. (2015). Three spectrally distinct photoreceptors in diurnal and nocturnal Australian ants. *Proc R Soc Biol Sci Ser B* **282**, 20150673.

Ogawa, Y., Ryan, L. A., Palavalli-Nettimi, R., Seeger, O., Hart, N. S. and Narendra, A. (2019). Spatial Resolving Power and Contrast Sensitivity Are Adapted for Ambient Light Conditions in Australian Myrmecia Ants. *Front. Ecol. Evo.* **7**.

Olivo, R. F. and Chrismer, K. L. (1980). Spectral sensitivity of screening-pigment migration in retinula cells of the crayfish Procambarus. *Vision Res.* **20**, 385-389.

Olivo, R. F. and Larsen, M. E. (1978). Brief exposure to light initiates screening pigment migration in retinula cells of the crayfish, Procambarus. *J. Comp. Physiol., A* **125**, 91-96.

Osorio, D. and Vorobyev, M. (2008). A review of the evolution of animal colour vision and visual communication signals. *Vision Res.* **48**, 2042-2051.

Rajkumar, P., Rollmann, S. M., Cook, T. A. and Layne, J. E. (2010). Molecular evidence for color discrimination in the Atlantic sand fiddler crab, Uca pugilator. *J. Exp. Biol.* **213**, 4240-4248.

Reddy, P., Fingerman, M., Nguyen, L. and Obih, P. (1997). Effect of cadmium chloride on the distal retinal pigment cells of the fiddler crab, Uca pugilator. *Bulletin of environmental contamination and toxicology* **58**.

Ribi, W. A. (1978). Ultrastructure and migration of screening pigments in the retina of Pieris rapae L.(Lepidoptera, Pieridae). *Cell Tissue Res.* **191**, 57-73.

Rosenberg, J., Henning, U. and Langer, H. (2000). Diurnal changes of fine structure in the compound eyes of the ghost crab Ocypode ryderi (Crustacea, Decapoda, Ocypodidae). *Acta Biol Benrodis* **11**, 53-70.

Rosenberg, J. and Langer, H. (2001). Ultrastructural changes of rhabdoms of the eyes of Ocypode species in relation to different regimes of light and dark adaptation. *J. Crust. Biol.* **21**, 345-353.

Ryan, L. A., Cunningham, R., Hart, N. S. and Ogawa, Y. (2020). The buzz around spatial resolving power and contrast sensitivity in the honeybee, Apis mellifera. *Vision Res.* **169**, 25-32.

Satoh, A., Stewart, F. J., Koshitaka, H., Akashi, H. D., Pirih, P., Sato, Y. and Arikawa, K. (2017). Red-shift of spectral sensitivity due to screening pigment migration in the eyes of a moth, Adoxophyes orana. *Zool. Lett.* **3**, 14.

Scott, S. and Mote, M. I. (1974). Spectral sensitivity in some marine Crustacea. *Vision Res.* **14**, 659-663.

Shaw, S. R. and Stowe, S. (1982). Photoreception. *Neurobiology: Structure and Function*, 291-367.

Shih, H.-T., Ng, P. K. L., Davie, P. J. F., Schubart, C. D., Türkay, M., Naderloo, R., Jones, D. and Liu, M.-Y. (2016). Systematics of the family Ocypodidae Rafinesque, 1815 (Crustacea: Brachyura), based on phylogenetic relationships, with a reorganization of subfamily rankings and a review of the taxonomic status of Uca Leach, 1814, sensu lato and its subgenera. *Raffles Bull. Zool.* **64**.

Smolka, J. (2009). Sampling visual space: topography, colour vision and visually guided predator avoidance in fiddler crabs (Uca vomeris). *PhD Thesis*, Australian National University, Canberra, ACT.

Stavenga, D. G. and Arikawa, K. (2011). Photoreceptor spectral sensitivities of the Small White butterfly Pieris rapae crucivora interpreted with optical modeling. *J. Comp. Physiol., A* **197**, 373-385.

Stowe, S. (1980). Spectral sensitivity and retinal pigment movement in the crab Leptograpsus variegatus (Fabricius). *J. Exp. Biol.* **87**, 73-98.

Stowe, S. (1982). Rhabdom synthesis in isolated eyestalks and retinae of the crabLeptograpsus variegatus. *J. Comp. Physiol., A* **148**, 313-321.

Toh, Y. (1987). Diurnal changes of rhabdom structures in the compound eye of the grapsid crab, Hemigrapsus penicillatus. *J Electron Microsc Tech* **36**, 213-223.

Tomsic, D., Pedreira, M. E., Romano, A., Hermitte, G. and Maldonado, H. (1998). Context-us association as a determinant of long-term habituation in the crabChasmagnathus. *Animal Learning & Behavior* **26**, 196-209.

Van Hateren, J. H. (1984). Waveguide theory applied to optically measured angular sensitivities of fly photoreceptors. *Journal of Comparative Physiology A* **154**, 761-771.

Zeil, J. and Hofmann, M. (2001). Signals from ‘crabworld’: cuticular reflections in a fiddler crab colony. *J. Exp. Biol.* **204**, 2561-2569.

Figures

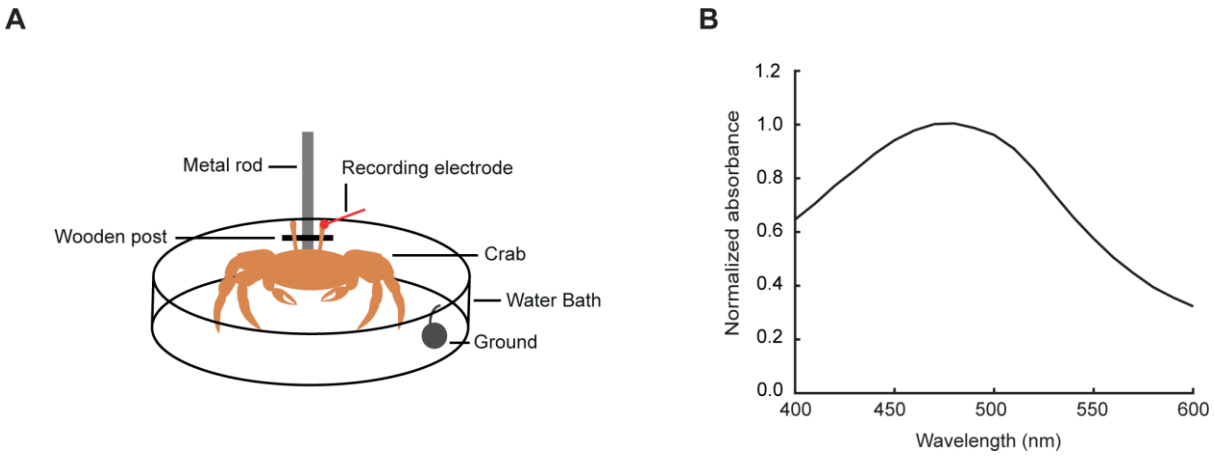

Figure 1. Electrophysiological recording setup and screening pigment absorbance spectrum. (a) The crab was held by gluing its carapace to a metal rod and the eye stalks in their natural positions to a wooden post. A shielded silver/silver chloride pellet was placed inside the sea water bath containing the crab and served as the recording ground. For ERG measurements, differential recordings were made between the platinum wire placed onto the stimulated eye and the pellet placed inside the sea water bath. For intracellular measurements the silver/silver chloride pellet served as the indifferent electrode and a glass microelectrode was inserted into the stimulated eye. (b) Normalised absorbance spectrum of the *G. vomeris* screening pigment from Jordão et al. (2007) that was included in the optical modelling.

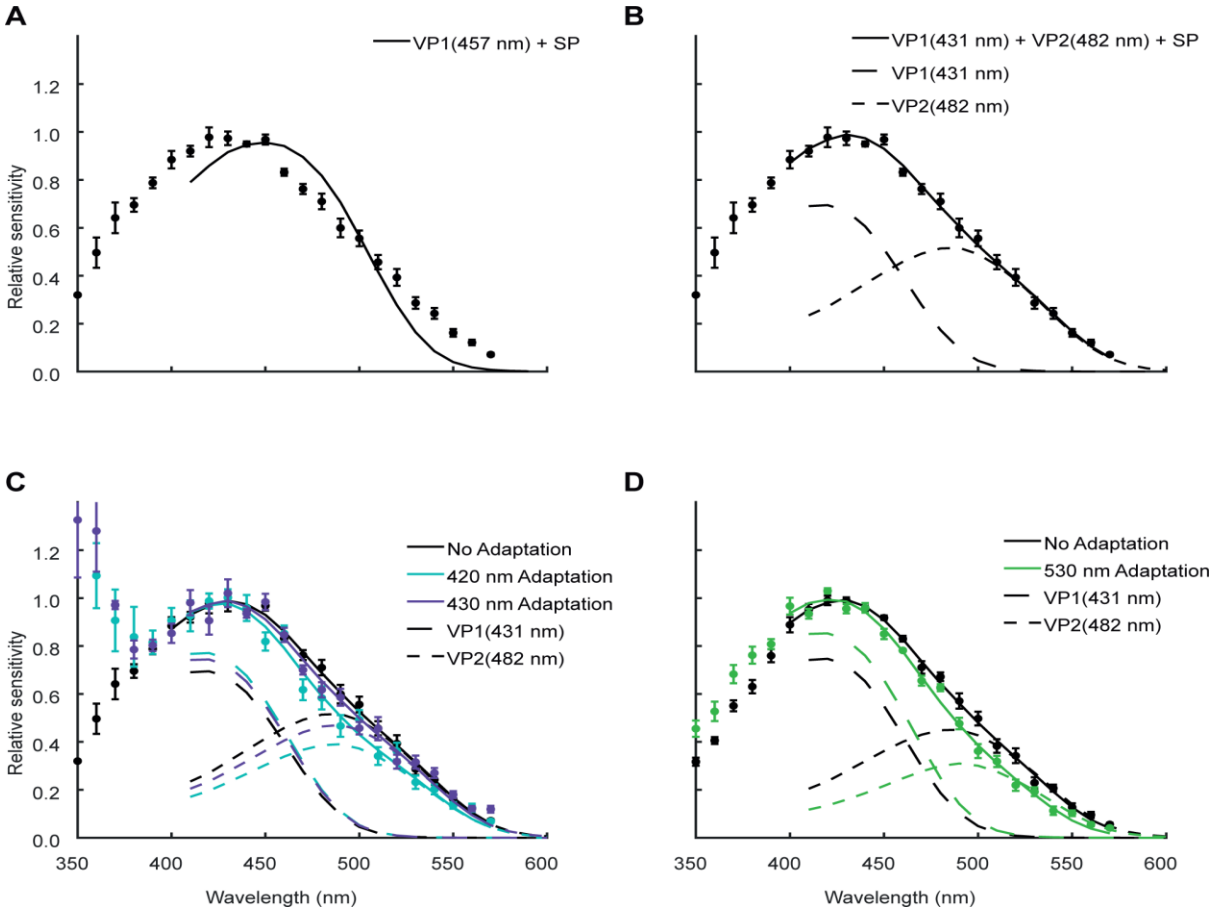

Figure 2. Spectral responses from the eye of the fiddler crab *G. dampieri* recorded by ERG under different experimental conditions fitted with optical models. (a) Optical model including one visual pigment (VP1) and the *G. vomeris* screening pigment (SP) (Jordão et al., 2007) (b) Optical model including two visual pigments (VP1 and VP2) and the *G. vomeris* screening pigment (SP). (c) Best fitting model from (b) with only the relative contribution of each visual pigment being unconstrained fitted to the spectral responses from the eye under the no adaptation, 420 nm adaptation and 430 nm adaptation conditions. (d) Best fitting model from (b) with only the relative contribution of each visual pigment being unconstrained fitted to the spectral responses from the eye under the no adaptation and 530 nm adaptation conditions. In all figures the optical models are displayed as solid curves and the mean spectral response data are displayed as circles (mean ± SEM, N = 5). VP1 and VP2 absorbance spectra, after screening pigment effects are factored in, are displayed in their relative contributions for each condition, shown as dashed curves. Mean data were calculated by scaling the raw data to the mean model for each condition.

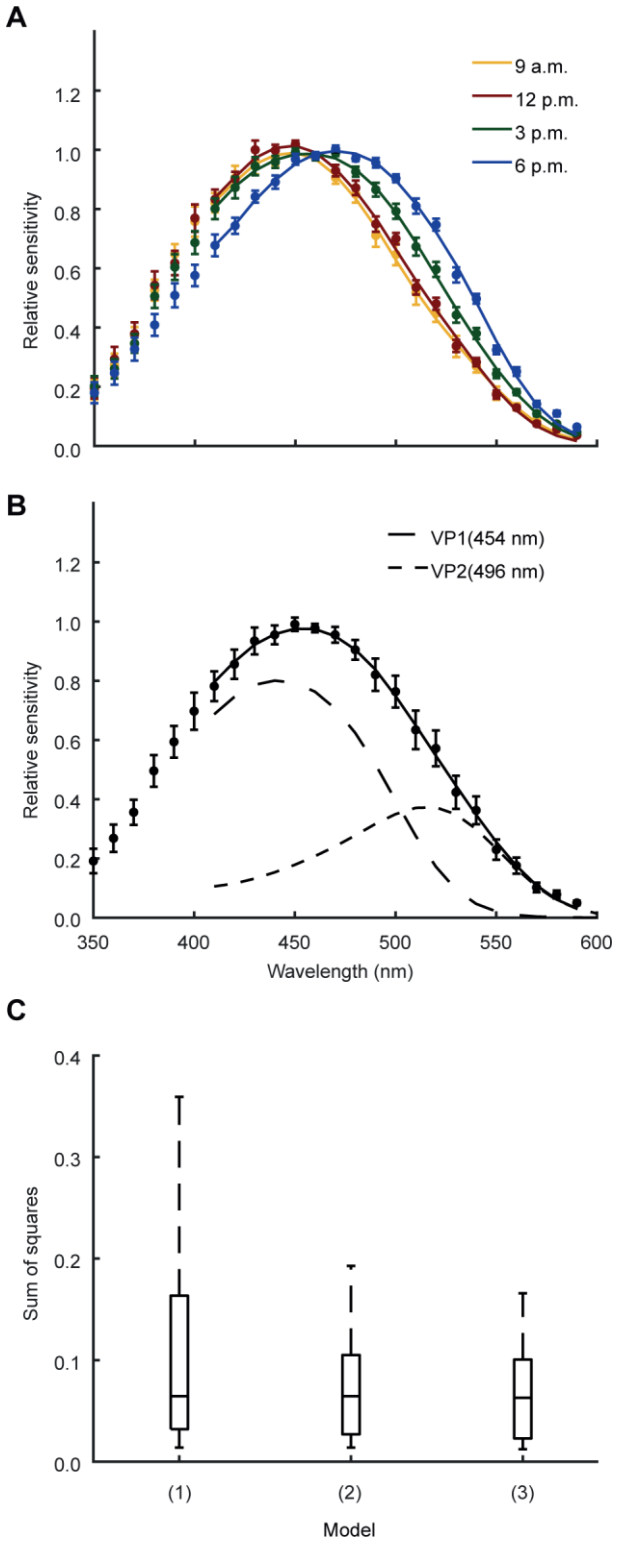

Figure 3. Mean ERG recordings taken at four different times of day and the distribution of error between three different models and spectral responses. (a) Mean ERG recordings, displayed as circles (mean ± SEM, N = 8), from eight *G. dampieri* individuals, made at four different times of day. Each curve shows the best fitting model for each time. (b) Mean of all ERG recordings, displayed as circles (mean ± SEM, N = 8) with the best fitting model displayed

as the black curve. Dashed curves display the visual pigment templates after screening pigment effects that were incorporated into the model. (c) The median sum of squares error is almost identical between the three models ((1) Screening pigment migration $\tilde{x}$ = 0.0645, (2) Opsin regulation $\tilde{x}$ = 0.0645, (3) Combination $\tilde{x}$ = 0.0629), however the range of the screening pigment migration model is slightly higher than the other two models, indicating the model does not fit all times of the day equally well.

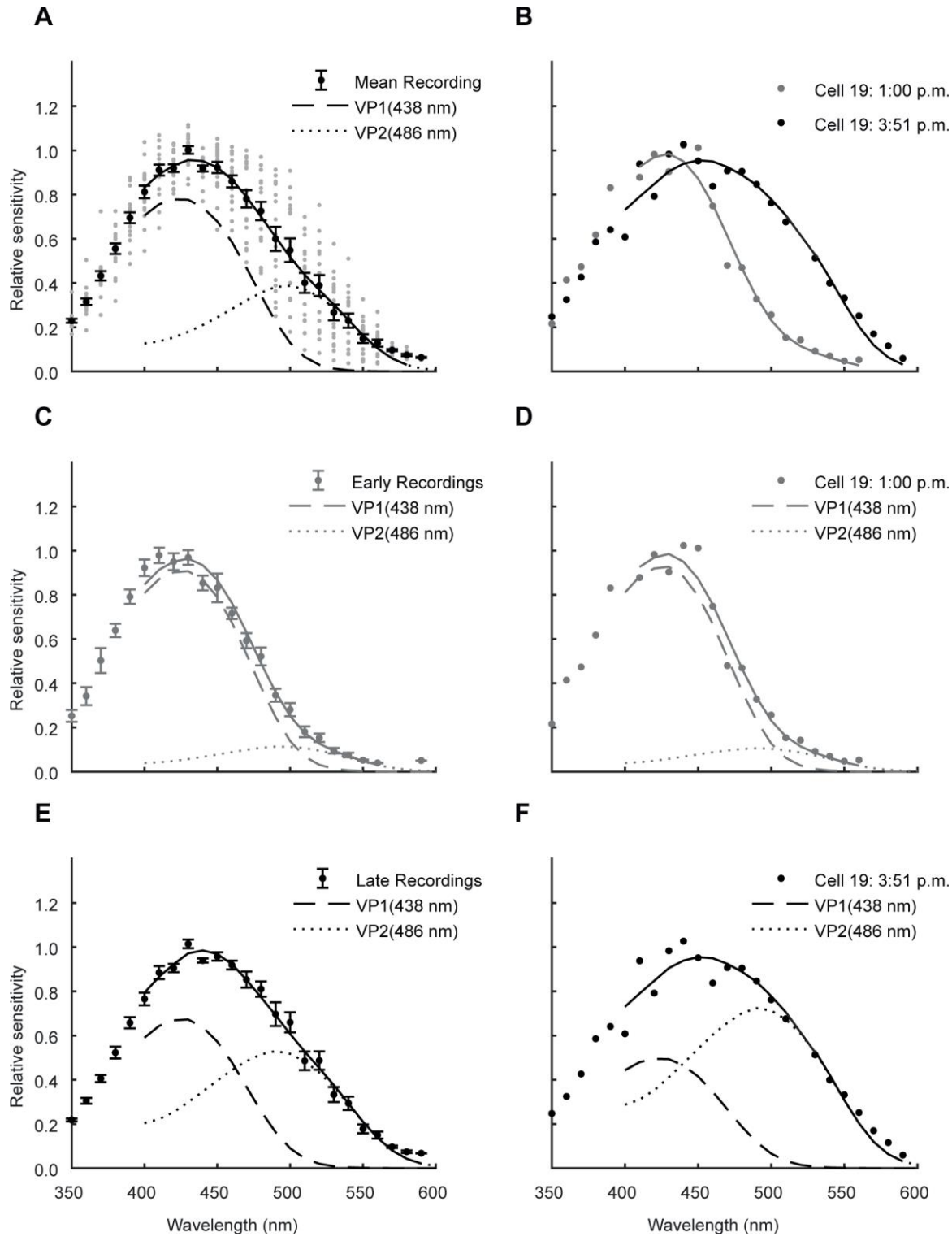

Figure 4. Intracellular recordings from *G. dampieri* retinular cells. (a) Spectral responses from all retinular cells (grey dots) with the mean response ± SEM (black circles) and the mean model (black line) fitted to all responses. (b) Spectral responses of Cell 19 at 1:00 p.m. and 3:51 p.m. fitted with the mean model from (a), but with only the λ_{max} of each visual pigment constrained. Grey circles show data recorded at 1:00 p.m. and black circles show data recorded

at 3:51 p.m. (c) Mean spectral response from early cells (mean ± SEM, N = 5) fitted with the mean model in (a). (e) Mean spectral response from late cells (mean ± SEM, N = 13) fitted with the mean model in (a). (d) Spectral response from Cell 19 at 1:00 p.m. fitted with the mean model in (a). (f) Spectral response from Cell 19 at 3:51 p.m. fitted with the mean model in (a). Dashed lines show the best fitting visual pigment templates after the effects of the screening pigment incorporated into the models in their relative contributions. In all panels solid lines show the best fitting optical model for the data.

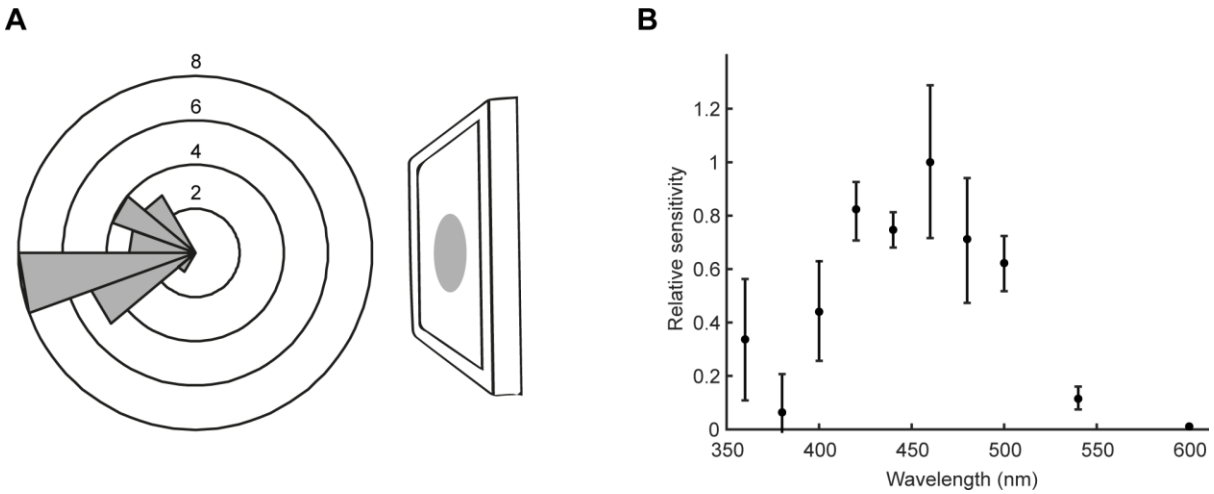

Figure 5. Spectral sensitivity of the escape behaviour of *G. dampieri*. (a) The direction of 'sprint' behaviours in response to the stimulus. Concentric circles represent the number of responses and the bin width is 20°. The stimulus is shown to the right of the polar histogram demonstrating the direction of the behaviour. (b) Mean relative spectral sensitivity of the escape response of *G. dampieri* displayed as black circles (mean ± SEM). For all test wavelengths except 360 nm and 380 nm N = 4, but for 360 nm and 380 nm N = 2.

Tables

Table 1. Model results for each of the adaptation conditions.

Condition	*p_i ratio VP1:VP2
No Adaptation	0.53:0.47
420 nm	0.63:0.37
430 nm	0.58:0.42
530 nm	0.68:0.32

***VP1:** visual pigment 1 (431 nm)**, VP2:** visual pigment 2 (482 nm)**,** p_i **ratio**: occupancy (contribution) ratio of visual pigments**.** The average time of day for each condition was 12:56 p.m. (no adaptation condition), 1:17 p.m. (420 nm condition), 2:02 p.m. (430 nm condition) and 1:15 p.m. (530 nm condition).

Table 2. Michelson's contrasts between the invariable white light and dark of the flickering stimulus that putative visual pigments identified by the optical model would have experienced under each condition.

Adaptation Light	350 nm visual pigment	431 nm visual pigment	482 nm visual pigment	Combined 431 nm and 482 nm visual pigments
No adaptation	100.0%	100.0%	100.0%	100.0%
420 nm	5.8%	0.5%	1.3%	0.8%
430 nm	17.6%	0.5%	1.1%	0.7%
530 nm	100.0%	22.6%	1.0%	1.6%

Table 3. Best fitting model parameters for each time of day.

Time	VP1 λ_{max} (nm)	VP2 λ_{max} (nm)	p_i ratio VP1:VP2	$k_{s,max}$
9 a.m.	449	489	0.68:0.32	0.021
12 p.m.	444	483	0.53:0.47	0.037
3 p.m.	450	498	0.73:0.27	0
6 p.m.	443	487	0.27:0.73	0.09

***VP1:** visual pigment 1**, VP2:** visual pigment 2**,** p_i **ratio**: occupancy (contribution) ratio of visual pigments, $k_{s,max}$**:** screening pigment absorbance coefficient

Table 4. Best fitting model parameters for each dataset show an increased contribution (p_i) of VP1 (438 nm) and decreased contribution of VP2 (486 nm) in early cells compared to late cells.

Dataset	VP1 λ_{max} (nm)	VP2 λ_{max} (nm)	p_i ratio VP1:VP2	$k_{s,max}$
Mean	438	486	0.68:0.32	0.01
Early Cells	438	486	0.89:0.11	0.032
Late Cells	438	486	0.53:0.47	0.0789
Cell 19 at 1:00 p.m.	438	486	0.89:0.11	0.1
Cell 19 at 3:51 p.m.	438	486	0.37:0.63	0.03

Supplementary Material

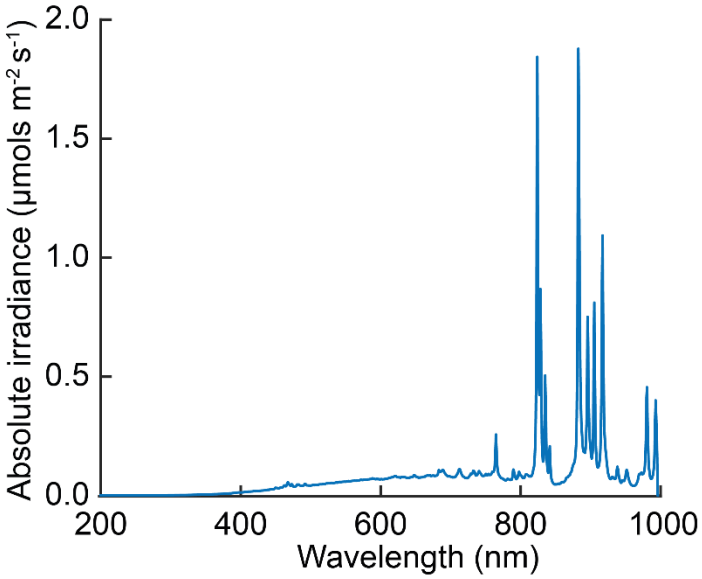

Figure S1. Spectrum of HPX-2000 that was used as the invariant white light in all experiments. The spectrum was measured using a spectrometer (QE *Pro*, Ocean Optics Inc., FL, USA) and the spectroscopy software OceanView (Ocean Optics Inc., FL, USA). The light from the HPX-2000 was delivered to the spectrometer via a fibre optic that passed light through a fibre optic variable attenuator (FVA-UV, Ocean Opitcs Inc., FL, USA) and finally to the HPX-2000 via a second fibre optic. The variable attenuator was set such that the light delivered to the spectrometer was of an intensity within the readable range of the spectrometer.

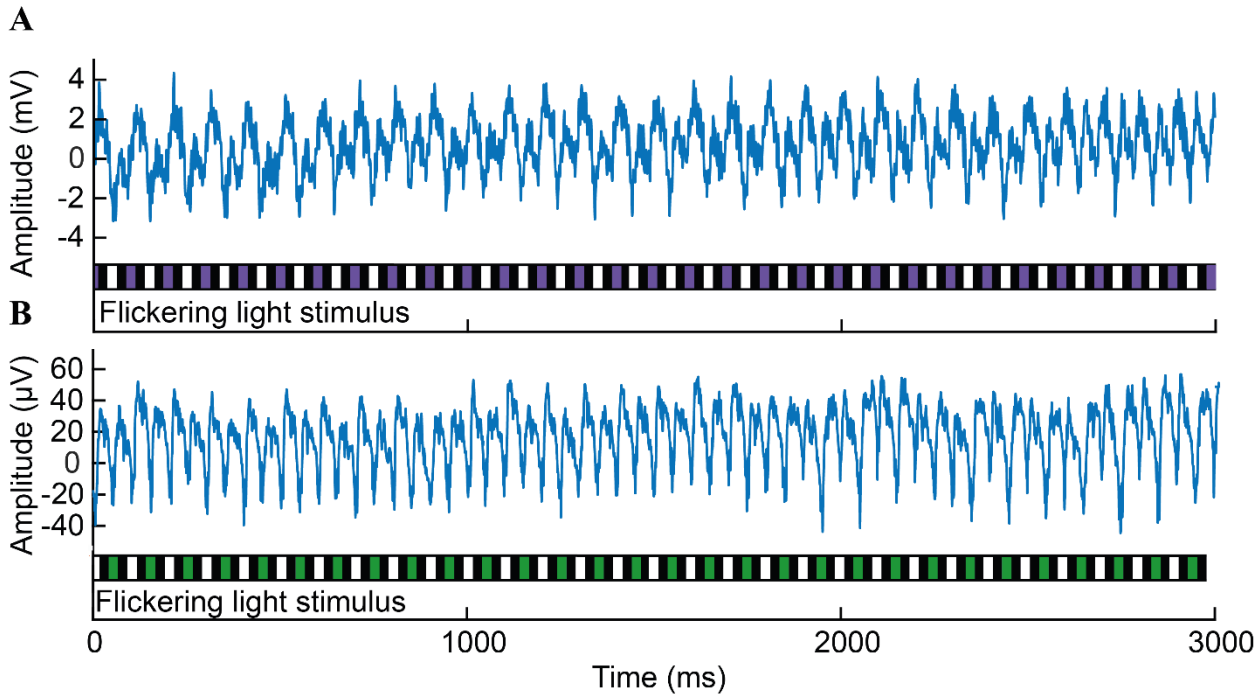

Figure S2. ERG and intracellular signal over three seconds of recording in response to a flickering light stimulus. (a) Filtered intracellular signal is displayed in blue and the amplitude of the response is before amplification. The raw intracellular signal was filtered with a 50 Hz notch filter and a low pass filter with a 70 Hz cutoff frequency. (b) A raw ERG signal is displayed in blue and the amplitude of the response is before amplification. In both figures the flickering light stimulus is displayed below the signal showing the invariant white light, followed by no light, followed by a coloured light, followed by no light. In (a) the coloured light was a 380 nm light that produced a weaker response than the invariant white light and in (b) the coloured light was a 530 nm light that produced approximately the same response as the invariant white light. In both intracellular and ERG recordings, responses to the light were delayed by approximately 60 ms.

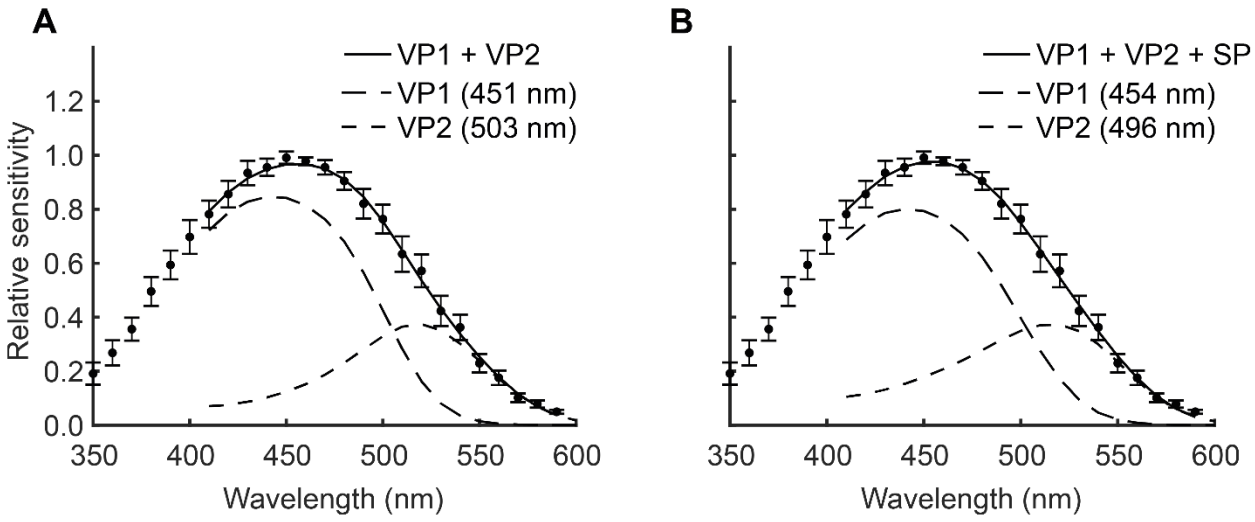

Figure S3. Mean ERG recordings from all times of day for *G. dampieri* fitted with a model excluding a screening pigment and including a screening pigment. (a) Mean ERG recordings fitted with a model excluding a screening pigment. (b) Mean ERG recordings fitted with a model including a screening pigment with an absorbance coefficient of 0.005 (mean ± SEM, N = 8). Model fit is displayed as a black curve and dashed curves show the two visual pigments in their relative contributions.

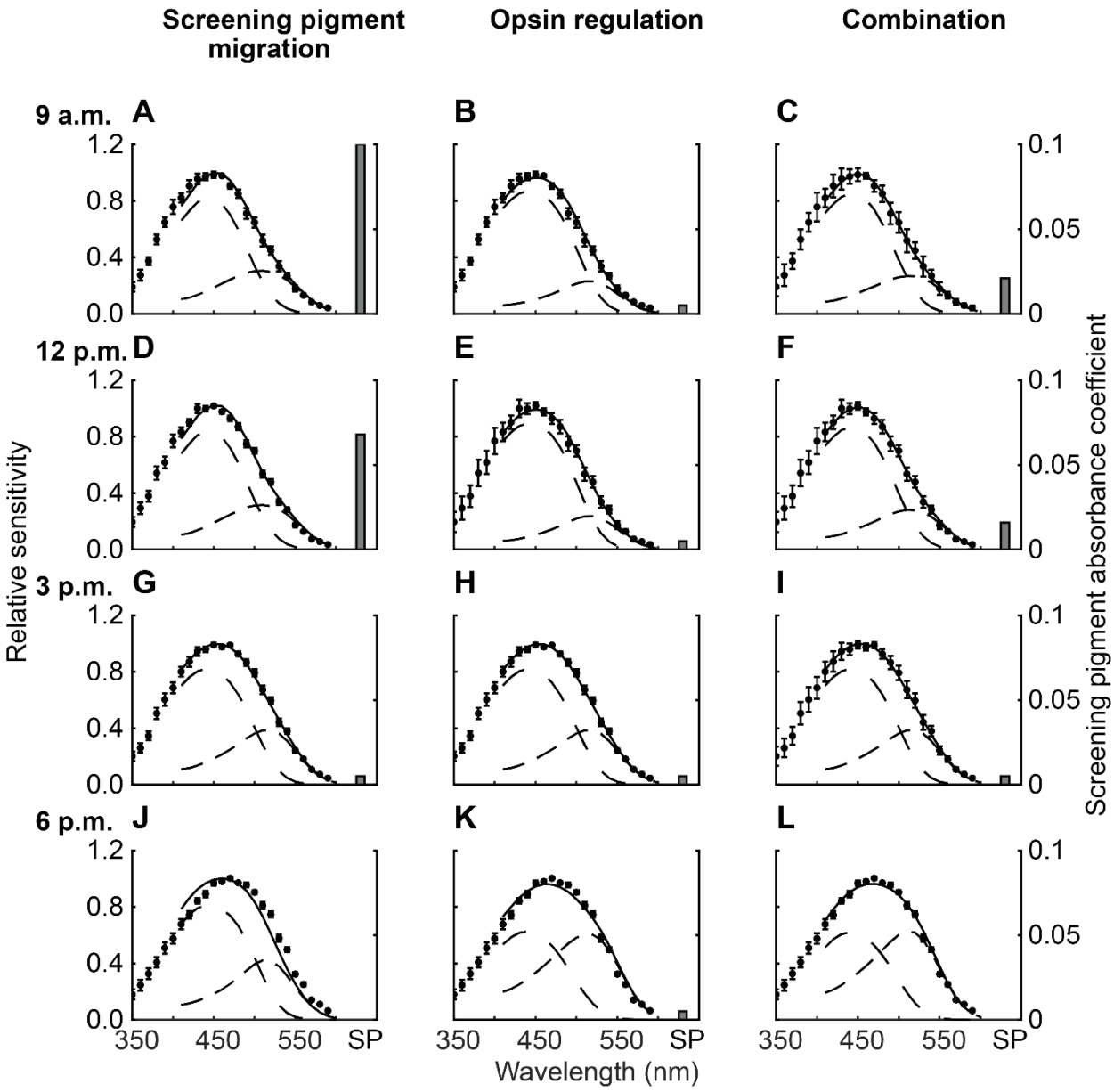

Figure S4. Mean ERG recordings from eight *G. dampieri* at 9 a.m., 12 p.m., 3 p.m., and 6 p.m., fitted with three different models. Mean ERG recordings (left y axis) are displayed as points (mean ± SEM, N = 8) and each model is displayed as the black curve. Dashed curves show the visual pigment templates after screening pigment effects for VP1 (454 nm) and VP2 (496 nm) in their relative contributions as shown in Table S1. Grey bars represent the screening pigment absorbance coefficient for each model (right y-axis).

Table S1. Best fitting model results for each of the three models fitted to the dataset from each time of day.

Model	Time	p_i ratio VP1:VP2	$k_{s,max}$
Screening pigment migration	9 a.m.	0.73:0.27	**0.1**
	12 p.m.	0.73:0.27	**0.068**
	3 p.m.	0.73:0.27	**0.005**
	6 p.m.	0.73:0.27	**0**
Opsin regulation	9 a.m.	**0.84:0.16**	0.005
	12 p.m.	**0.84:0.16**	0.005
	3 p.m.	**0.73:0.27**	0.005
	6 p.m.	**0.53:0.47**	0.005
Combination	9 a.m.	**0.78:0.22**	**0.021**
	12 p.m.	**0.78:0.22**	**0.016**
	3 p.m.	**0.73:0.27**	**0.005**
	6 p.m.	**0.53:0.47**	**0**

Supplementary Material

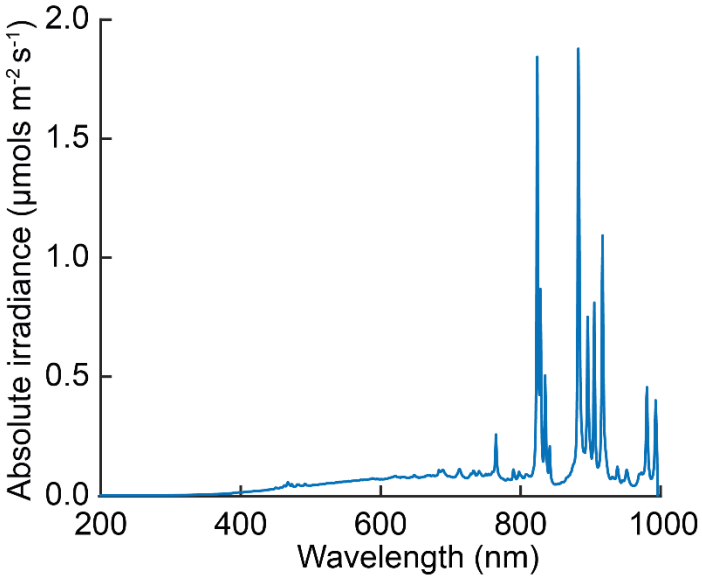

Figure S1. Spectrum of HPX-2000 that was used as the invariant white light in all experiments. The spectrum was measured using a spectrometer (QE *Pro*, Ocean Optics Inc., FL, USA) and the spectroscopy software OceanView (Ocean Optics Inc., FL, USA). The light from the HPX-2000 was delivered to the spectrometer via a fibre optic that passed light through a fibre optic variable attenuator (FVA-UV, Ocean Opitcs Inc., FL, USA) and finally to the HPX-2000 via a second fibre optic. The variable attenuator was set such that the light delivered to the spectrometer was of an intensity within the readable range of the spectrometer.

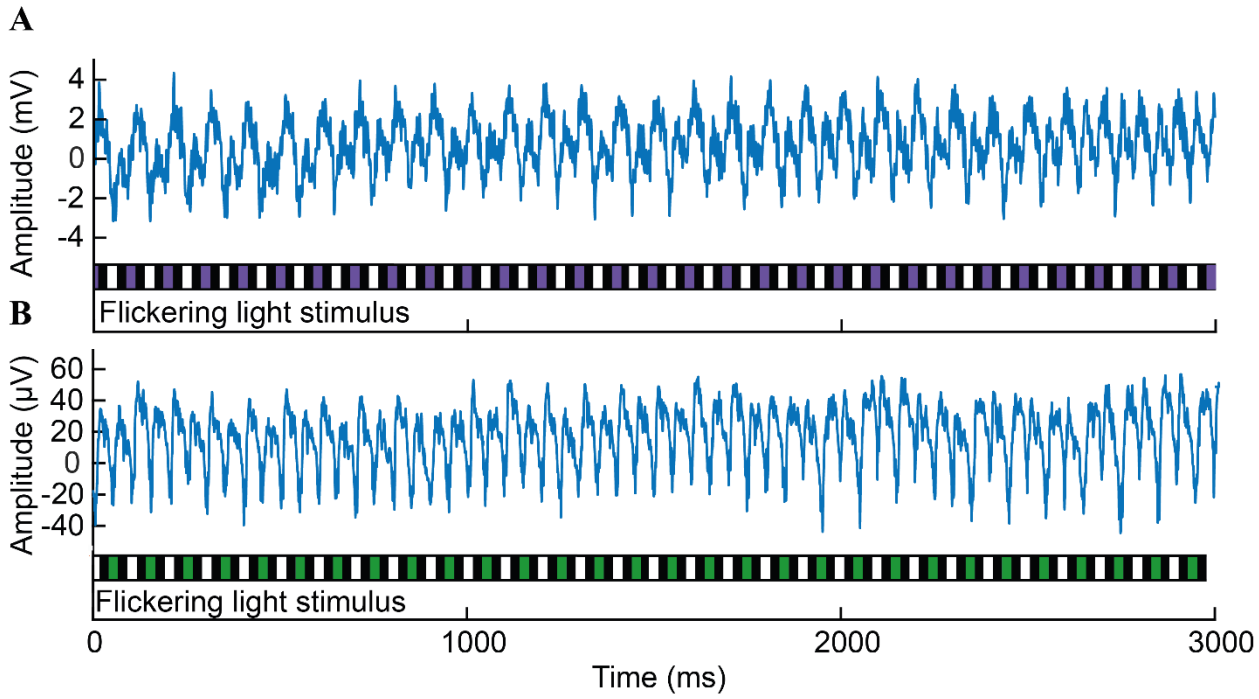

Figure S2. ERG and intracellular signal over three seconds of recording in response to a flickering light stimulus. (a) Filtered intracellular signal is displayed in blue and the amplitude of the response is before amplification. The raw intracellular signal was filtered with a 50 Hz notch filter and a low pass filter with a 70 Hz cutoff frequency. (b) A raw ERG signal is displayed in blue and the amplitude of the response is before amplification. In both figures the flickering light stimulus is displayed below the signal showing the invariant white light, followed by no light, followed by a coloured light, followed by no light. In (a) the coloured light was a 380 nm light that produced a weaker response than the invariant white light and in (b) the coloured light was a 530 nm light that produced approximately the same response as the invariant white light. In both intracellular and ERG recordings, responses to the light were delayed by approximately 60 ms.

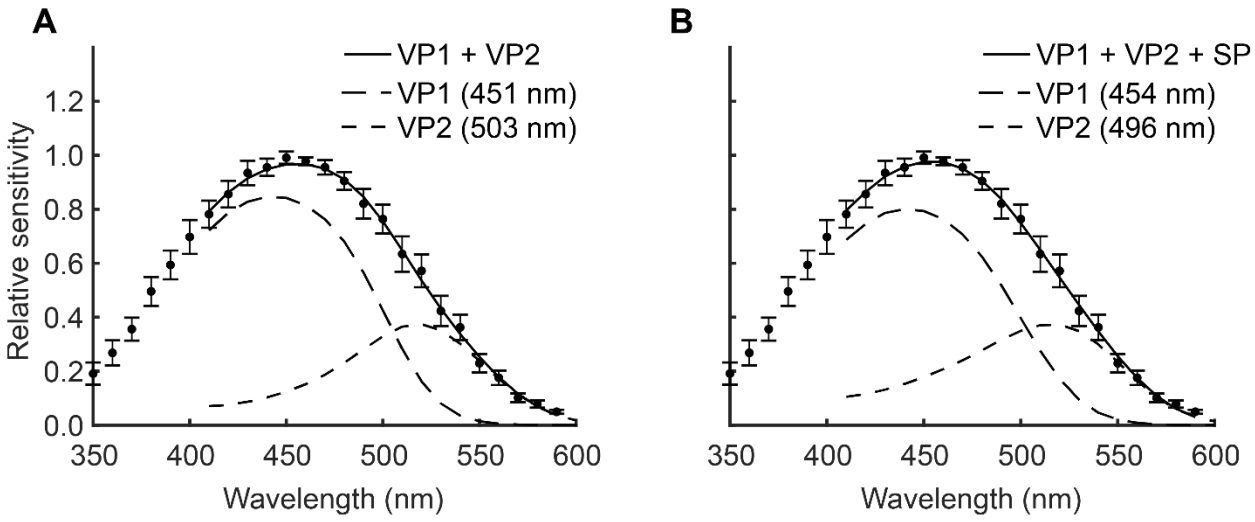

Figure S3. Mean ERG recordings from all times of day for *G. dampieri* fitted with a model excluding a screening pigment and including a screening pigment. (a) Mean ERG recordings fitted with a model excluding a screening pigment. (b) Mean ERG recordings fitted with a model including a screening pigment with an absorbance coefficient of 0.005 (mean ± SEM, N = 8). Model fit is displayed as a black curve and dashed curves show the two visual pigments in their relative contributions.

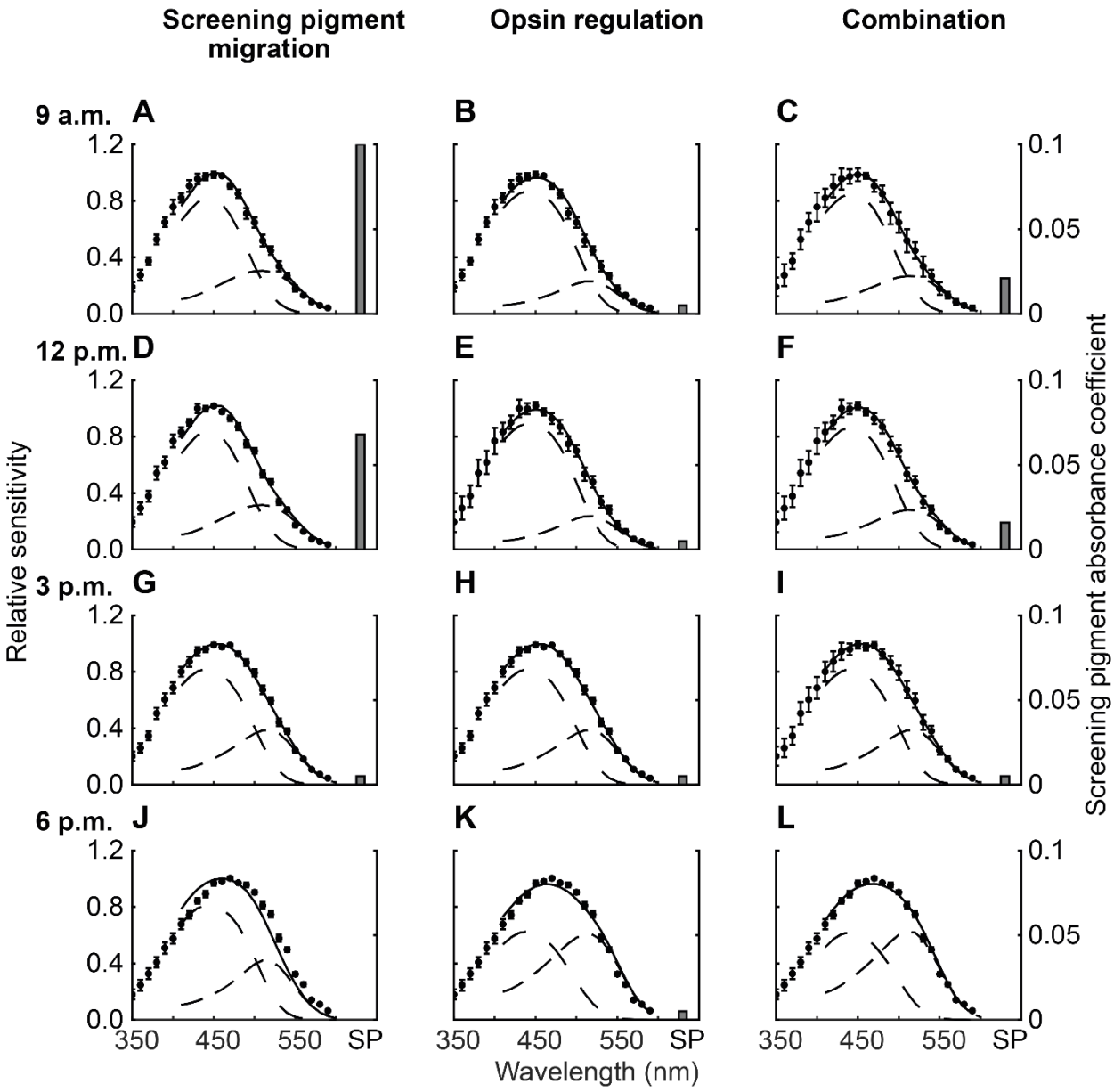

Figure S4. Mean ERG recordings from eight *G. dampieri* at 9 a.m., 12 p.m., 3 p.m., and 6 p.m., fitted with three different models. Mean ERG recordings (left y axis) are displayed as points (mean ± SEM, N = 8) and each model is displayed as the black curve. Dashed curves show the visual pigment templates after screening pigment effects for VP1 (454 nm) and VP2 (496 nm) in their relative contributions as shown in Table S1. Grey bars represent the screening pigment absorbance coefficient for each model (right y-axis).

Table S1. Best fitting model results for each of the three models fitted to the dataset from each time of day.

Model	Time	p_i ratio VP1:VP2	$k_{s,max}$
Screening pigment migration	9 a.m.	0.73:0.27	**0.1**
	12 p.m.	0.73:0.27	**0.068**
	3 p.m.	0.73:0.27	**0.005**
	6 p.m.	0.73:0.27	**0**
Opsin regulation	9 a.m.	**0.84:0.16**	0.005
	12 p.m.	**0.84:0.16**	0.005
	3 p.m.	**0.73:0.27**	0.005
	6 p.m.	**0.53:0.47**	0.005
Combination	9 a.m.	**0.78:0.22**	**0.021**
	12 p.m.	**0.78:0.22**	**0.016**
	3 p.m.	**0.73:0.27**	**0.005**
	6 p.m.	**0.53:0.47**	**0**